Structured uncertainty analysis of pole placement and H_∞ controllers for directional drilling attitude tracking

M. T. Bayliss * **J. F. Whidborne** ** **N. Panchal** *

* *Schlumberger Oilfield UK Plc. (e-mail: mbayliss@slb.com, npanchal@slb.com).*
** *School of Engineering, Cranfield University, Bedfordshire, MK43 OAL, UK*
(e-mail: j.f.whidborne@cranfield.ac.uk)

Abstract: This paper describes the design of attitude-hold controllers and their subsequent stability and performance analysis for directional drilling tools as typically used in the oil industry. Based on an input transformation developed in earlier work that partially linearizes and decouples the plant dynamics of the drilling tool, the resulting plant model is used as the basis for both a pole placement (as detailed in previous work) and optimal H_∞ controller designs. A structured uncertainty stability and performance analysis is then performed on each of the two controller designs. Results for a transient simulation of the proposed controller are also presented.

Keywords: Robust control, optimal, linear, feedback, attitude control, drilling.

1. INTRODUCTION

In recent years the oil and gas industry has sought to extend the life of existing wells and to exploit smaller and hitherto difficult-to-commercialize reservoirs by using directional drilling and rotary steerable drilling tools (Pedersen et al., 2009). Steerable tools enable the direction of the well propagation to be directed as required either by passive steering control from the surface using fixed-bend positive displacement motors (Tetsuo et al., 2002; Kuwana et al., 1992) or by steering the wellbore propagation downhole using a rotary steerable system (RSS) drilling tool. Directional drilling, by either approach, is essentially attitude control, i.e., concerned with controlling azimuth and inclination (Genevois et al., 2003).

This paper extends work on a generic (tool-independent) attitude-control algorithm previously developed for use with directional drilling tools (Panchal et al., 2010). The importance of attitude control is highlighted by Genevois et al. (2003) and Tetsuo et al. (2002) who propose control strategies for the direction of wellbore propagation based on holding the tool-face angle. Genevois et al. (2003) discuss the need for closed-loop 'shoot and forget systems' and state that the major challenge has been azimuth control. Many of the attitude control strategies presented in the literature are discussed in the context of specific tool architectures; Tetsuo et al. (2002), Genevois et al. (2003) and Liu and Su (2000) are typical examples. Another interesting example is by Kuwana et al. (1992) who describe a system for controlling attitude using two-way telemetry communication links with the surface; the steering correction, evaluated from the telemetry, is computed and then manually downlinked to the tool.

In the previous work (Panchal et al., 2010) a controller was detailed that has the control objective, once engaged, of automatically holding the inclination and azimuth of the tool at nominally constant values as the well propagates. Usually the tool is manually controlled to the desired location and orientation, the attitude (azimuth and inclination) is measured, and then these values are subsequently used as the demand attitude for the control algorithm. An analysis of the robust stability of the controller using the small gain theorem is performed. Here, the work is extended by consideration of structured uncertainty. Structured singular value stability and performance analysis are performed on both the earlier pole placement controller and an H_∞ optimal controller. The optimal H_∞ control design is included as a bench mark for comparison with the pole placed design and appropriate conclusions are stated at the end of the paper. The paper also includes a description and results from time domain simulations for the two control designs for typical operating point parameters and uncertainties.

The paper is structured so that the design methodologies for the pole placement and H_∞ control designs are presented, starting with a statement of the plant model used for subsequent structured singular value stability and performance analysis, and, finally, incorporating it into a transient simulation using the plant model in nonlinear form together with the necessary control architecture. For reference the 'off line' control design and analysis was performed using MATLAB and its associated Robust Control Toolbox commands and the subsequent 'on line' transient simulations were performed in Simulink.

2. SUMMARY OF EARLIER WORK

2.1 Tool Kinematics

The plant model is derived from kinematic considerations as detailed in Panchal et al. (2010). The resulting governing equations can be stated as follows:

$$\dot{\theta}_{\mathrm{inc}} = V_{\mathrm{rop}} \left(U_{\mathrm{dls}} \cos U_{\mathrm{tf}} - V_{\mathrm{dr}} \right) \tag{1}$$

$$\dot{\theta}_{\mathrm{azi}} = \frac{V_{\mathrm{rop}}}{\sin \theta_{\mathrm{inc}}} \left(U_{\mathrm{dls}} \sin U_{\mathrm{tf}} - V_{\mathrm{tr}} \right), \tag{2}$$

where

θ_{inc} is the inclination angle
θ_{azi} is the azimuth angle
U_{tf} is the tool-face angle control input
U_{dls} is the curvature ($K_{\mathrm{dls}} \times$ duty cycle)
K_{dls} is the open loop curvature capability of the tool
V_{dr} is the drop rate disturbance ($V_{\mathrm{dr}} = \alpha \sin \theta_{\mathrm{inc}}$)
V_{tr} is the turn rate bias disturbance
V_{rop} is the rate of penetration and is an uncontrolled
        parameter.

Note the subscript *dls* has been used to reflect that in the oil industry curvature is often referred to as 'dogleg severity'. The tool-face dynamics are significant, and although they are not included in the plant nominal model, their effect is taken into account in a structured uncertainty analysis. As detailed in Panchal et al. (2010) the engineering considerations that the control inputs U_{dls} and U_{tf} are discretised into duty cycles known as 'drilling cycles' and the tool-face input U_{tf} is subject to first order lag dynamics should be considered. The actuation drilling cycles can be abstracted as pure delays for analysis purposes. Additionally, the on-tool feedback measurements of θ_{inc} and θ_{azi} are subject to pure delays dependent on V_{rop} as a consequence of the relevant sensors being spatially offset from the drill bit (the inertial datum).

2.2 Uncoupled and Linearized Plant

The MIMO open loop plant can be linearized and uncoupled using the following transformation:

$$U_{\mathrm{tf}} = \mathrm{ATAN2}\left(U_{\mathrm{azi}}, U_{\mathrm{inc}}\right) \qquad (3)$$

$$U_{\mathrm{dls}} = K_{\mathrm{dls}}\sqrt{\left(U_{\mathrm{azi}}\right)^2 + \left(U_{\mathrm{inc}}\right)^2}, \qquad (4)$$

where U_{azi} and U_{inc} are virtual control of azimuth and inclination, respectively. Linearizing about an operating point $\hat{\theta}_{\mathrm{inc}}$, $\hat{\theta}_{\mathrm{azi}}$, the open-loop plant given by (1) and (2) can be formulated as follows:

$$\dot{x}_{\mathrm{inc}} = a u_{\mathrm{inc}} \qquad (5)$$

$$\dot{x}_{\mathrm{azi}} = c x_{\mathrm{inc}} + b u_{\mathrm{azi}}, \qquad (6)$$

where $a = V_{\mathrm{rop}} K_{\mathrm{dls}}$, $b = a\alpha_1$, $c = -a\alpha_1\alpha_2$, $\alpha_1 = \csc\ \hat{\theta}_{\mathrm{inc}}$ and $\alpha_2 = \cot\ \hat{\theta}_{\mathrm{inc}}$. Taking the output to be $y = [x_{\mathrm{inc}}, x_{\mathrm{azi}}]^T$, the nominal transfer function is then

$$G_0(s) = \begin{bmatrix} \frac{a}{s} & 0 \\ \frac{ac}{s^2} & \frac{b}{s} \end{bmatrix}. \qquad (7)$$

This can be factorized into

$$G_0 = G_{\mathrm{i1}} G_0' G_{\mathrm{i2}} \qquad (8)$$

$$= \begin{bmatrix} 1 & 0 \\ 0 & \frac{1}{s} \end{bmatrix} \begin{bmatrix} a & 0 \\ -a^2\alpha_1\alpha_2 & a\alpha_1 \end{bmatrix} \begin{bmatrix} \frac{1}{s} & 0 \\ 0 & 1 \end{bmatrix}. \qquad (9)$$

3. CONTROL DESIGN

The proposed scheme for both the pole placement and H_∞ controller designs is shown in Fig. 1. For both design methodologies, the nominal plant G_o is used and the actuator and measurement dynamics are ignored.

3.1 Pole Placement Design

The PI controller for each channel is

$$u_{\mathrm{inc}} = k_{\mathrm{pi}} e_{\mathrm{inc}} + k_{\mathrm{ii}} \int_0^t e_{\mathrm{inc}} dt \qquad (10)$$

$$u_{\mathrm{azi}} = k_{\mathrm{pa}} e_{\mathrm{azi}} + k_{\mathrm{ia}} \int_0^t e_{\mathrm{azi}} dt, \qquad (11)$$

where $e_{\mathrm{inc}} = r_{\mathrm{inc}} - x_{\mathrm{inc}}$ and $e_{\mathrm{azi}} = r_{\mathrm{azi}} - x_{\mathrm{azi}}$. It is shown in Panchal et al. (2010) that the gains for the PI controllers
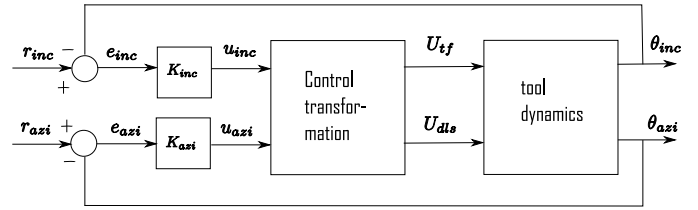

Fig. 1. Control scheme

in the SISO azimuth and inclination feedback loops as functions of the ω_a and ω_i natural frequencies and gain-scheduled V_{rop} and K_{dls} operating points can be expressed as:

$$k_{\mathrm{ii}} = \frac{\omega_i^2}{a}, \qquad k_{\mathrm{pi}} = \frac{\sqrt{2}\omega_i}{a}, \qquad (12)$$

$$k_{\mathrm{ia}} = \frac{\omega_a^2}{b}, \qquad k_{\mathrm{pa}} = \frac{\sqrt{2}\omega_a}{b}. \qquad (13)$$

3.2 H_∞ Controller Design

The H_∞ controller design is achieved by formulating the problem in a standard way as shown in Fig. 2 where the standard form description can be realized as:

$$\begin{bmatrix} z \\ v \end{bmatrix} = \begin{bmatrix} P_{11} & P_{12} \\ P_{21} & P_{22} \end{bmatrix} \begin{bmatrix} w \\ u \end{bmatrix},$$

where:

$$P_{11} = \begin{bmatrix} W_1 \\ 0 \end{bmatrix}, \qquad P_{12} = \begin{bmatrix} -W_1 G \\ W_2 G \end{bmatrix}, \qquad (14)$$
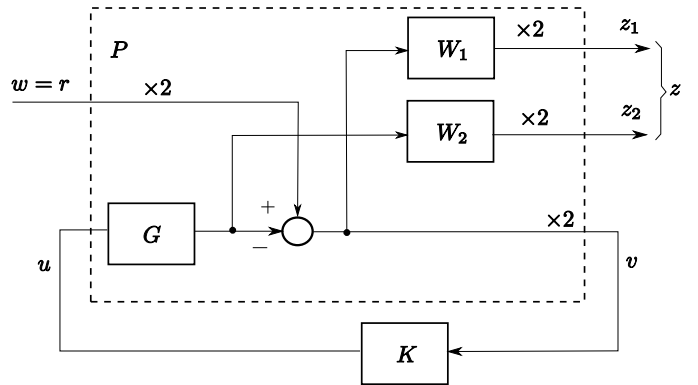
$$P_{21} = I, \qquad P_{22} = -G. \qquad (15)$$

Fig. 2. S/T mixed-sensitivity standard form (Skogestad and Postlethwaite, 2005)

This can be posed as an H_∞ optimal control problem:

$$\min_{\mathrm{stabilizing}\ K} \left\| \begin{bmatrix} W_1 S \\ W_2 T \end{bmatrix} \right\|_{\infty}, \qquad (16)$$

where the sensitivity and tracking performance objectives are stacked to achieve a mixed sensitivity design approach. The weighting functions W_1 and W_2 for the sensitivity and tracking performance are of the form:

$$W_1(s) = \frac{\left(s/M^{1/n} + \omega_B^*\right)^n}{\left(s + \omega_B^* A^{1/n}\right)^n}, \qquad (17)$$

$$W_2(s) = \frac{\left(s + \omega_B^* A^{1/n}\right)^n}{\left(s/M^{1/n} + \omega_B^*\right)^n} \qquad (18)$$

where A is the low/high frequency gain, M is the high/low frequency gain and ω_B^* are the bandwidths for S and T, respectively. The parameters A, M and ω_B^* need not be the same for both performance weightings. For both, n dictates the $(\omega_B/s)^n$ slope of the performance asymptotes. Performance weightings W_1 and W_2 and their parameters are used to tune the competing system sensitivity and tracking performances and hence lead to the performance specification for the control system using the H_∞ controller design approach.

The H_∞ optimal control design approach tends to result in high order controllers and for practical implementation reasons require model reduction as detailed by Safonov and Chiang (1988). In this paper, the Hankel singular values for the MIMO controller were computed and an order reduction from 10 to 4 was applied and then the reduced order design passed through a structured singular value analysis to show robustness. The same approach of 'design and then analyze' has also been used for the pole placement. Future work will include direct robust control where the control design will ensure robustness in one step.

Table 1. Controller design specifications

Specification	Value
Pole placement θ_{inc} frequency	1.05×10^{-2} rad/sec
Pole placement θ_{azi} frequency	1.26×10^{-2} rad/sec
Pole placement damping ratio	0.707
H_∞ W_1 M high frequency gain	1.6
H_∞ W_1 A low frequency gain	0.2
H_∞ W_1 ω_b^* bandwidth	2.0×10^{-2} rad/sec
H_∞ W_1 n order	2
H_∞ W_2 M low frequency gain	1.0
H_∞ W_2 A high frequency gain	0.2
H_∞ W_2 ω_b^* bandwidth	1.0×10^{-2} rad/sec
H_∞ W_2 n order	2
ω specification range	$1.0 \times 10^{-6} \to 1.0 \times 10^{-3}$ rad/sec

4. UNMODELED DYNAMICS

Using either of the methodologies given in section 3, it is possible to design the four feedback gains to ensure nominal stability and performance at a given plant operating point. However, for each design operating point, for a given set of gains, it is also important to assess the robust stability and performance of the design. When the lags and delays are combined with the tool dynamics and the controller, the open-loop system becomes:

$$L(s) = G_1(s)K(s), \tag{19}$$

where $G_1(s) = H_2(s)G_0(s)H_1(s)H_{lag}(s)$ is the model for the actual plant, and

$$H_i(s) = h_i(s)\begin{bmatrix} 1 & 0 \\ 0 & 1 \end{bmatrix} \tag{20}$$

where $i = 1, 2, lag$, with

$$h_1(s) = \frac{1 - s\lambda_1}{1 + s\lambda_1}, \qquad h_2(s) = \frac{1 - s\lambda_2}{1 + s\lambda_2} \tag{21}$$

$$h_{lag}(s) = \frac{1}{1 + s\tau_d}, \tag{22}$$

respectively. A block diagram representation of $G_1(s)$ is shown in Fig. 3.

In order to meet the requirement for the application of structured singularity analysis, the actual plant model is taken to be $G_1(s) = G_0(s) + \Delta(s)$ where $G_0(s)$ is the nominal plant given by (7) and $\Delta(s)$ is the structured uncertainty arising from the stated parametric uncertainties.
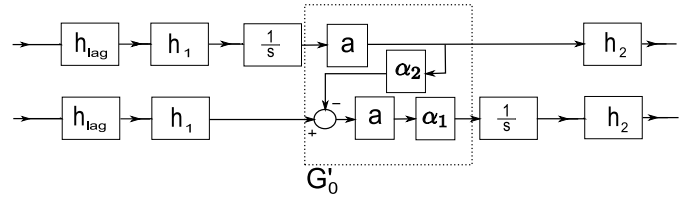

Fig. 3. Open-loop plant $G_1(s)$ with the integrators factored out of the nominal plant
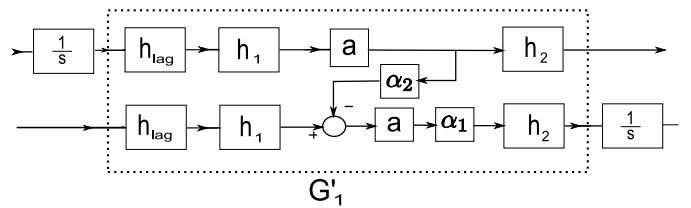

Fig. 4. Open loop plant with integrators factored outside

Because the delays and lag are scalar functions, the integrators in the plant can be factored outside the plant as shown in Fig. 4, and this is represented by:

$$G_1(s) = G_{i1}(s)G_1'(s)G_{i2}(s) \tag{23}$$

where: $G_{i1}(s) = diag(1, \frac{1}{s})$,
$G_1'(s) = H_2(s)G_0'(s)H_1(s)H_{lag}(s)$ and $G_{i2}(s) = diag(\frac{1}{s}, 1)$.
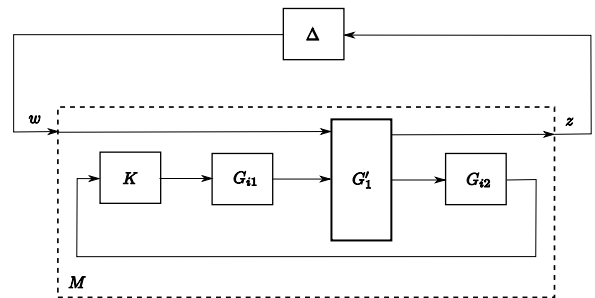

Fig. 5. $M\Delta$ structure

Since $G_{i1}(s)$ and $G_{i2}(s)$ can be factored outside the plant, they can be extracted from the uncertainty to give the $M\Delta$ robust stability structure as described by Skogestad and Postlethwaite (2005) and shown in Fig. 5. Further, the $M\Delta$ structure can be augmented by pulling out the sensitivity and tracking outputs factored by the normalising weighting transfer functions $W_1(s)$ and $W_2(s)$, respectively, as shown in Fig. 6.

The $M\Delta$ structures shown in Figs. 5 and 6 can then be used in conjunction with the real bounded lemma to establish the uncertainty bounds for the structured singular value over the frequency range of interest (Doyle, 1982; Safonov, 1982). Of note is the normalization of the Δ uncertainty block by uncertainty weightings factored into the M matrix enabling the pulled-out uncertainty to have $\|\Delta\|_\infty \leq 1$, $\forall \omega$. The normalization of the Δ block enables the structured singular value bound β criterion (stability or mixed) to be be stated as

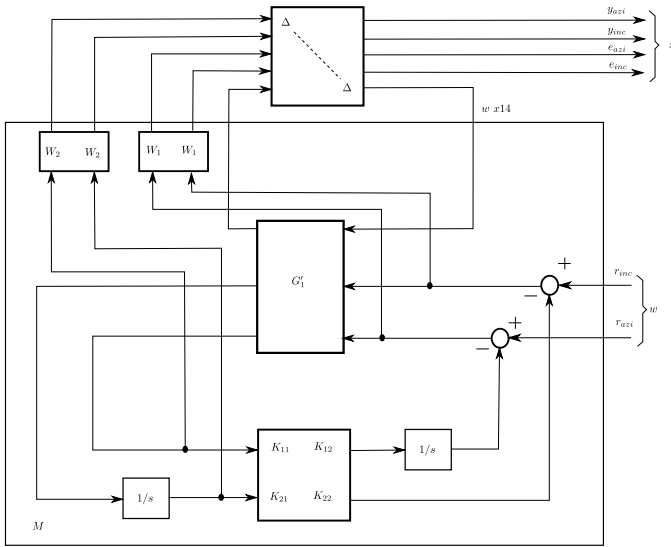$$\frac{1}{\beta} > \max_\omega \bar{\sigma}[\Delta(j\omega)] > 1, \tag{24}$$

Fig. 6. Mixed sensitivity augmented $M\Delta$ structure

for any structured uncertainty perturbation such that $\Delta \in \mathbf{\Delta}$, where $\mathbf{\Delta}$ denotes the set of all Δ. In order to pull out the structured real scalar parametric uncertainty in the open-loop stable subplant G_1', upper linear fractional transforms (LFTs) (Packard, 2013) were used as shown in Fig. 7 on the next page . Note that the delay and lag parametric uncertainties used the block substructures as detailed in Packard (2013) with the parametric uncertainties being the delay γ and time constant τ terms.

In the analysis performed for this paper, the normalizing uncertainty weighings for the real uncertainties shown pulled out in Fig. 7 were as shown in Table 2.

Table 2. Uncertainty range parameters

$\delta = W\Delta$	Nominal	Real uncertainty	units
δ_{γ_1}	360	180	s
δ_τ	10	2.5	s
δ_k	1	0.1	-
$\delta_{V_{\rm rop}}$	100	50	ft/hr
$\delta_{K_{\rm dls}}$	5	0.5	°/100 ft
δ_{α_1}	0	1.75×10^{-2}	-
δ_{α_2}	1	1	-
δ_{γ_2}	180	45	s

With reference to Table 2, note that for the csc and cot parameters the nominal operating inclination of 90° with a $\pm 1.0°$ perturbation were taken and the nominal and range for csc and cot evaluated accordingly. The feedback delay γ_1 was evaluated assuming the nominal $V_{\rm rop}$ and a spatial delay of 10 ft. The output quantization delay γ_2 was taken as half the assumed drilling cycle period of 360 seconds with a 25% uncertainty on the delay.

It can be seen in Fig. 7 that all the real scalar uncertainties except δ_{α_1} and δ_{α_2} are incorporated simultaneously in multiple instances within the G_1' structure. Therefore, for each structured singular value analysis, these simultaneous uncertainties were ordered within the M matrix normalizing weighting vector as follows:

$$W_\Delta = \begin{bmatrix} W_{\gamma_1} I_{2\times2}, & W_\tau I_{2\times2}, & W_k I_{2\times2}, & W_{V_{\rm rop}} I_{2\times2}, \\ W_{K_{\rm dls}} I_{2\times2}, & W_{\alpha_1}, & W_{\alpha_2}, & W_{\gamma_2} I_{2\times2} \end{bmatrix}^T \tag{25}$$

5. μ ANALYSIS AND TRANSIENT SIMULATION RESULTS

Two transient simulations were run using the nonlinear plant model given by (1) and (2) for the operating point and parameter set listed in Table 3 for the pole placement and H_∞ controllers, respectively, whose design specifications are listed in Table 1.

Table 3. Transient model parameters

Parameter	Value
Nominal attitude $\theta_{\rm inc}$, $\theta_{\rm azi}$	90° and 270°
Nominal $K_{\rm dls}$	5°/100 ft
Disturbance drop rate	1°/100 ft
Disturbance turn rate	0.5°/100 ft
Nominal $V_{\rm rop}$	100 ft/hr
Drilling cycle	360 s
Actuation 1st order time constant	10 s
Parametric uncertainties	see Table 2

5.1 μ Analysis Results

Fig. 8 shows the μ stability analysis results for the pole placement and H_∞ designed controllers, respectively. Similarly, Fig. 9 shows the μ mixed sensitivity analysis results for the pole placement and H_∞ designed controllers, respectively. For both stability and both mixed sensitivity analysis plots it can be seen that the criteria are met such that both the upper and lower μ bounds are less than unity and hence predict stable systems meeting the performance criteria implied by the $W_1(s)$ and $W_2(s)$ weighting functions over the frequency range of interest.
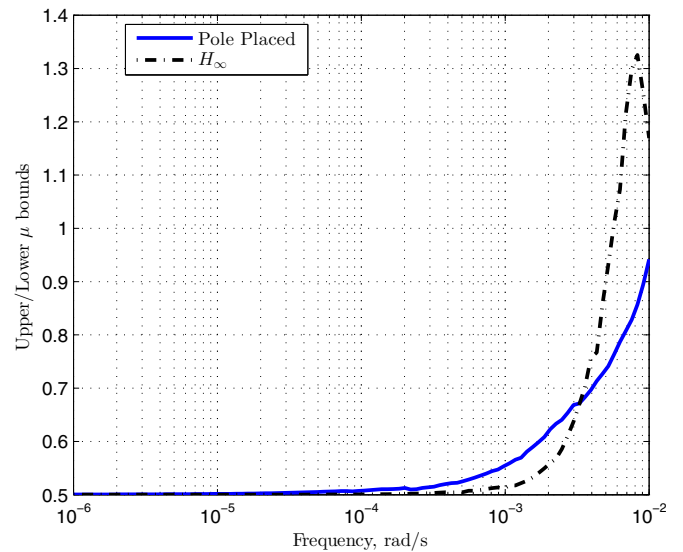

Fig. 8. μ stability analysis

It is also worth noting that the stability and mixed sensitivity analysis results for both the pole placement and H_∞ controllers are, in fact, similar. Although the H_∞ margin is better as the upper frequency range, though both design methods pass the mixed sensitivity criterion over the full frequency range (stated in Table 1).

5.2 Transient Simulation Results

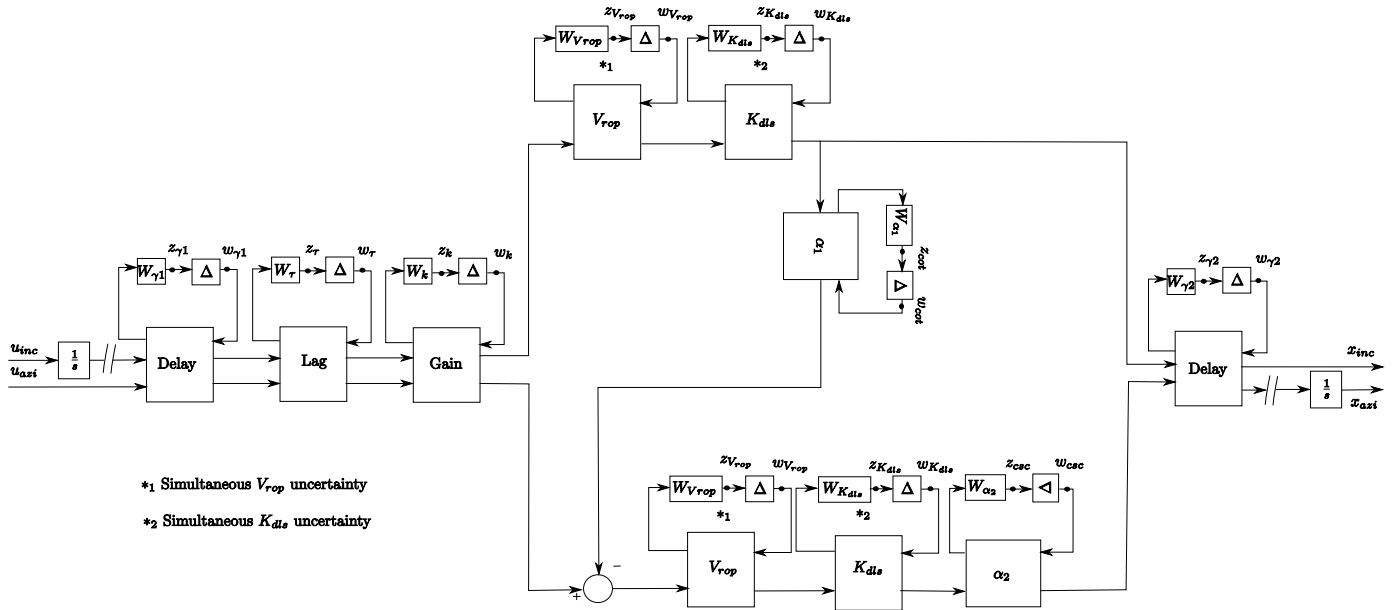Fig. 10 shows the transient attitude response for the pole placement controller design, and it can be seen that the

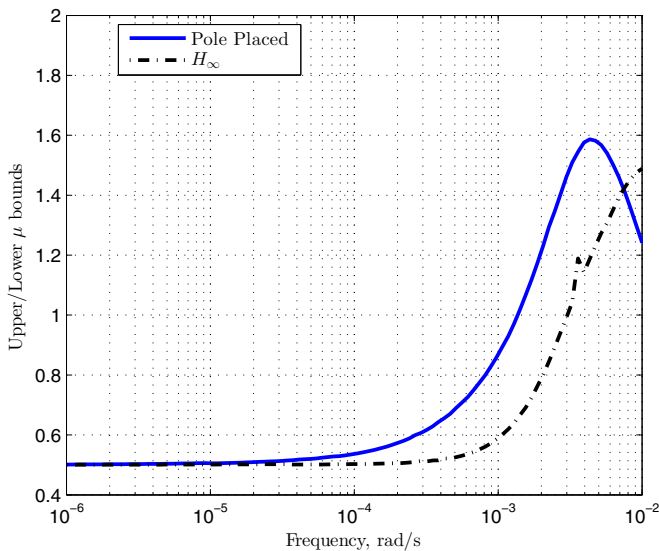Fig. 7. Internal G'_1 uncertainty structure

Fig. 9. μ mixed sensitivity analysis

controller tracked the initial 90° and 270° θ_{inc} and θ_{azi}, respectively to within ±0.8°, which can also be seen in the state trajectory error plot shown in Fig. 12. It was observed that the transient simulation responses for both the pole placement and H_∞ controllers were near identical as would be expected from the similarly near-identical μ analysis results.

It is also of note that for both the pole placement and H_∞ controllers, the control actuation was saturated on one of the two control outputs, namely U_{dls}, implying the steering ratio was at 100% for the whole simulation, whilst the other output, the actuating tool face u_{tf}, varied as shown in Fig. 11 (note zoomed view in Fig. 12 with the first order response evident). This implies that with a high gain setting, the pole placement and H_∞ controllers reduce to being identical in actuation and response to the discrete attitude controller detailed in Panchal et al. (2012). The behavior of the discrete, high-gain pole placement and H_∞

controllers is such that state response stays in a stable *limit cycle* when on target, as shown in Figs. 11, 12 and 13.
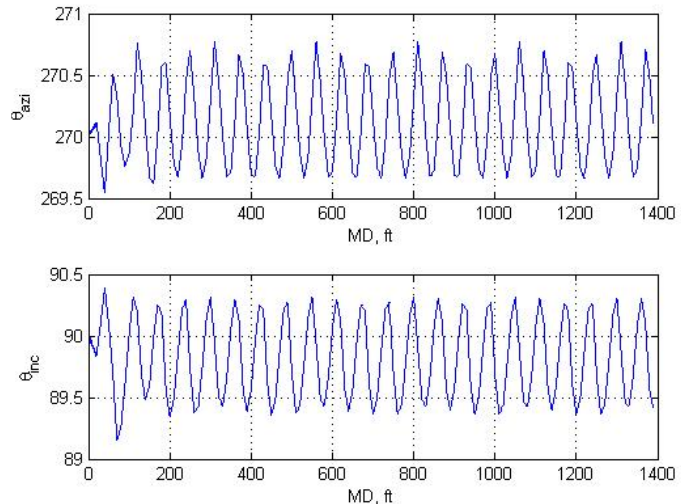

Fig. 10. Attitude tracking transient attitude response, pole placement design

6. CONCLUSION

This paper describes the design of two attitude controllers by means of pole placement and H_∞ methods and then, for a stated uncertainty and performance specification details, the subsequent μ stability and mixed sensitivity analysis. It is noted that the resulting μ analysis and transient simulation results are similar for both methods of controller design and that therefore the simpler and lower order pole placement design compares well against the more optimal bench marking H_∞ design. It was also noted that both controllers resulted in a saturated actuation on one of the two controller outputs and that therefore with high gain settings on these controllers they reduce to being identical in actuation and response to a discrete attitude controller previously detailed by the authors.
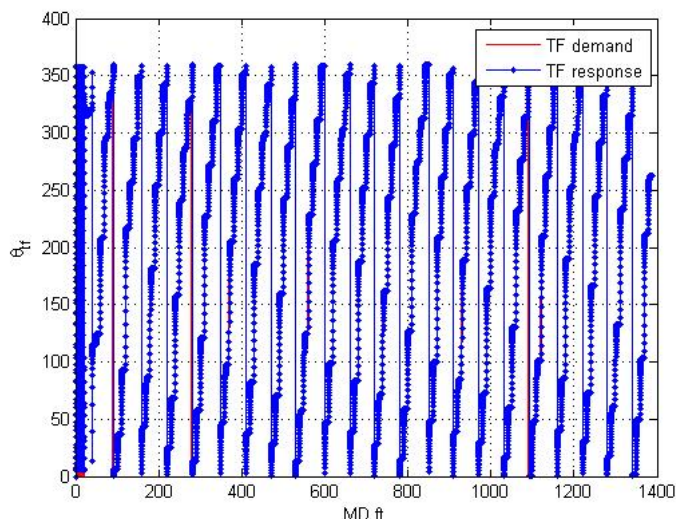
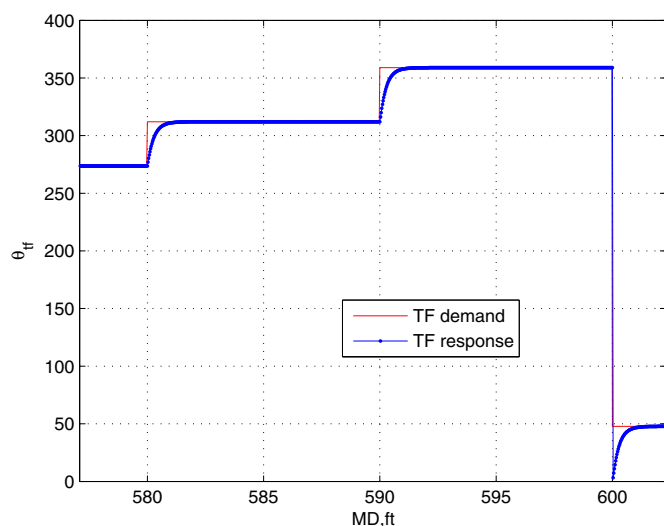Fig. 11. Attitude tracking transient actuator tool-face response, pole placement design

Fig. 12. Attitude tracking transient actuator tool-face response, pole placement design, zoomed view

Fig. 13. Attitude tracking transient state trajectory responses, pole placement design

REFERENCES

Doyle, J.C. (1982). Analysis of feedback systems with structured uncertainties. *IEE Proceedings-D*, 129(6), 242–250. doi:10.1049/ip-d:19820053.

Genevois, J.M., Boulet, J., Simon, C., and Reullon, C. (2003). Gyrostab project : The missing link azimuth and inclination mastered with new principles for standard rotary BHAs. In *Proc. IADC/SPE Drilling Conference*, SPE-79915-MS. SPE/IADC, Amsterdam, Netherlands. doi:10.2118/79915-MS.

Kuwana, S., Kiyosawa, Y., and Ikeda, A. (1992). Attitude control device and drilling-direction control device. Patent.

Liu, Y. and Su, Y. (2000). Automatic inclination controller: A new inclination controlling tool for rotary drilling. In *Proc. ADC/SPE Drilling Conference*, SPE-59259-MS. SPE/IADC, New Orleans, LA. doi: 10.2118/59259-MS.
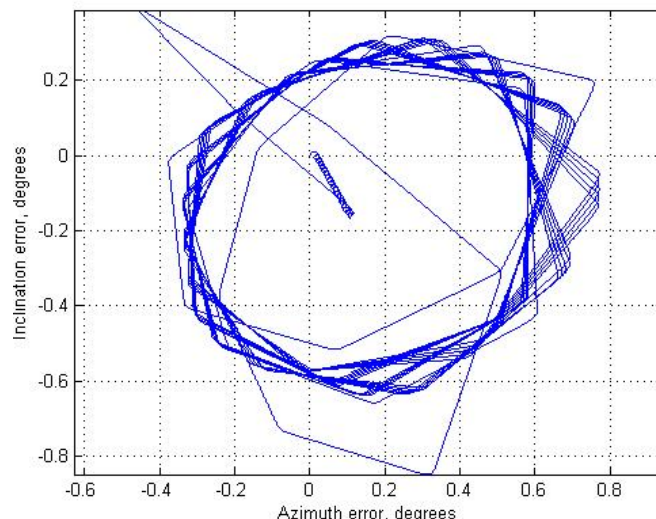
Packard, A. (2013). ME 234: Multivariable Control Systems – Uncertainty Modeling. Course notes. Mechanical Engineering, University of California, Berkeley.

Panchal, N., Bayliss, M.T., and Whidborne, J.F. (2010). Robust linear feedback control of attitude for directional drilling tools. In *Proc. 13th IFAC Symposium on Automation in Mining, Mineral and Metal Processing*. Cape Town, South Africa. doi:10.3182/20100802-3-ZA-2014.00022.

Panchal, N., Bayliss, M.T., and Whidborne, J.F. (2012). Attitude control system for directional drilling bottom hole assemblies. *IET Proceedings Control Theory and Applications*, 6(7), 884–892. doi:10.1049/iet-cta.2011.0438.

Pedersen, M.H., Lechner, M., Pon, Z.A., Brink, D., Abbasy, I., and Jaafar, M.R. (2009). Successful application of a novel conformance treatment in an extended reach horizontal well in the Al Shaheen field, offshore Qatar. In *Proc. Offshore Europe*, SPE-123949-MS. Aberdeen, UK. doi:10.2118/123949-MS.

Safonov, M.G. (1982). Stability margins of diagonally peturbed multivariable feedback systems. *IEE Proceedings-D*, 129(6), 251–256. doi:10.1049/ip-d:19820054.

Safonov, M.G. and Chiang, R.Y. (1988). Model reduction for robust control: A Schur relative error method. *International Journal of Adaptive Control and Signal Processing*, 2(4), 259–272. doi:10.1002/acs.4480020404.

Skogestad, S. and Postlethwaite, I. (2005). *Multivariable Feedback Control: Analysis and Design*. John Wiley, Chichester, U.K., second edition.

Tetsuo, Y., Cargill, E.J., Gaynor, T.M., Hardin, J., Hay, R.T., Akio, I., and Kiyosawa, Y. (2002). Robotic controlled drilling: A new rotary steerable drilling system for the oil and gas industry. In *Proc. IADC/SPE Drilling Conference*, SPE-74458-MS. SPE/IADC, Dallas, TX. doi:10.2118/74458-MS.